BIOCHEMISTRY
including biophysical chemistry & molecular biology

Article

pubs.acs.org/biochemistry

Identification of a Small Molecule PriA Helicase Inhibitor

Bharath Sunchu, Linda Berg, Hayley E. Ward, and Matthew E. Lopper*

Department of Chemistry, University of Dayton, 300 College Park, Dayton, Ohio 45469, United States

ABSTRACT: PriA helicase catalyzes the initial steps of replisome reloading onto repaired DNA replication forks in bacterial DNA replication restart pathways. We have used a high-throughput screen to identify a small molecule inhibitor of PriA-catalyzed duplex DNA unwinding. The compound, CGS 15943, targets *Neisseria gonorrhoeae* PriA helicase with an IC_{50} of 114 ± 24 μM. The PriA helicase of *Escherichia coli* is also inhibited, although to a lesser extent than *N. gonorrhoeae* PriA. CGS 15943 decreases rates of PriA-catalyzed ATP hydrolysis and reduces the affinity with which PriA binds DNA. Steady-state kinetic data indicate that CGS 15943 inhibits PriA through a mixed mode of inhibition with respect to ATP and with respect to DNA, indicating that it binds to a site on PriA that participates in both substrate binding and catalysis. Inhibitor binding constants derived from steady-state kinetic experiments reveal that CGS 15943 has the highest binding affinity for the PriA·PriB·ATP complex, intermediate binding affinity for the PriA·PriB·DNA complex, and the lowest binding affinity for the PriA·PriB·DNA·ATP complex, suggesting that PriA assumes different conformations in each of these complexes. We propose that CGS 15943 binds to PriA at a site distinct from the DNA and primary ATP binding sites, perhaps at PriA's weak nucleotide binding site, and induces a conformational change in PriA that renders it less catalytically proficient or prevents conformational changes in PriA that are necessary for ATP hydrolysis and duplex DNA unwinding.

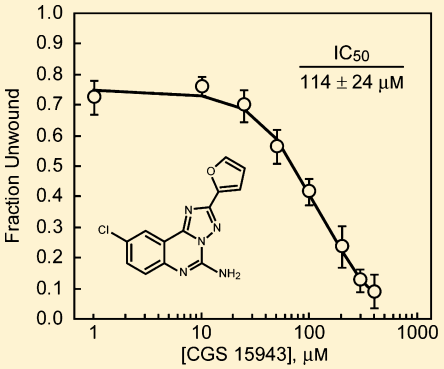

DNA damage creates barriers to the complete and faithful duplication of cellular genomes and, if not properly addressed, can lead to cell death.[1] In response to the ever-present threat of DNA-damaging agents, cells have evolved elaborate and highly effective mechanisms for detecting damaged DNA and either repairing or circumventing the damage to allow normal DNA metabolic processes to resume. In *Escherichia coli*, DNA replication forks that are disrupted because of encounters of the replication machinery (replisome) with damaged DNA are reactivated by DNA replication restart primosome proteins, including PriA helicase, PriB, PriC, DnaT, and Rep helicase.[2]

Genetic analysis of DNA replication restart in *E. coli* has revealed that the DNA replication restart primosome proteins function within multiple pathways: one pathway involves PriA, PriB, and DnaT, a second PriA, PriC, and DnaT, and a third Rep and PriC.[3,4] This model of multiple DNA replication restart pathways explains observations that null mutations in *priA*, *priB*, *priC*, and *dnaT* genes do not all display identical cellular phenotypes as would be expected for genes that operate in a single pathway.[4,5] Subsequently, two replisome reloading systems have been biochemically defined in *E. coli*: one that requires PriA, PriB, and DnaT and another that requires only PriC.[6] In vitro, these proteins are capable of reloading the replicative helicase, DnaB, onto an appropriately structured synthetic DNA template.[6] In vivo, the PriC-dependent pathway is also thought to require the DNA unwinding activity of either PriA helicase or Rep helicase.[3,7] The choice of which replisome reloading system a cell might use seems to be dictated by the type of DNA structure that requires reactivation: the PriA–PriB–DnaT pathway appears to be favored when the DNA fork has no gaps in the leading strand, while the PriC pathway appears to be favored when the DNA fork has large gaps in the leading strand.[6] Regardless of the pathway chosen, the overall goal of these replisome reloading systems is to facilitate the reloading of DnaB onto the DNA to allow continuation of DNA replication following a disruptive encounter of a replisome with a damaged DNA template.[2] The fact that *E. coli* harbors multiple DNA replication restart pathways likely underscores the importance of reactivating DNA replication forks that have diverse structures resulting from various genome maintenance processes.[2]

While many bacterial genomes lack obvious homologues of the *priB*, *priC*, and *dnaT* genes, the *priA* gene has been well conserved throughout evolution. Thus, DNA replication restart initiated by PriA helicase probably represents the major pathway of DNA replication restart in most bacteria. In *E. coli* cells, *priA* null mutations give rise to reduced cell viability, induction of the SOS response, and filamentous cell morphology, suggesting that these cells have defects in DNA replication and recombination.[8] Furthermore, *priA* null mutations are synthetically lethal with mutations that further disrupt genome stability, such as DNA gyrase and DNA polymerase mutations, lending additional support to the importance of *priA* in DNA replication restart pathways because these strains would have an increased requirement to reactivate repaired DNA replication forks.[9,10] PriA has been

Received: August 14, 2012
Revised: November 15, 2012
Published: November 29, 2012

shown to play an important role in genome maintenance in other bacteria; *Neisseria gonorrhoeae priA* plays a critical role in DNA repair and in resisting the toxic effects of oxidative damaging agents, and *priA* from *Neisseria meningitidis* has been identified as an important virulence determinant and is important for resisting oxidative injury and promoting bacterial replication.[11,12]

In vivo, PriA helicase is thought to initiate reactivation of repaired DNA replication forks by binding to specific DNA structures, such as forked DNA with three-way branches and D-loop DNA.[13,14] After binding to an appropriate DNA structure, PriA can catalyze unwinding of short stretches of duplex DNA using its 3′−5′ helicase activity and facilitate assembly of the remaining primosome proteins such as PriB and DnaT.[14−17] PriB is a primosome protein that binds to PriA and stabilizes PriA on the DNA.[14] PriB also simulates PriA's helicase activity and is thought to participate in recruiting DnaT to the primosome complex.[18−20] The combined activities of PriA, PriB, and DnaT facilitate recruitment of the DnaB−DnaC complex to the repaired DNA replication fork and the subsequent reloading of DnaB onto the DNA by an as yet unknown mechanism.[2]

PriA is a superfamily II helicase that comprises two structurally separable functional domains: an amino-terminal DNA-binding domain (DBD) and a carboxyl-terminal helicase domain (HD) that includes seven conserved helicase motifs.[21−23] The helicase motifs include a nucleotide-binding Walker A motif (also known as a phosphate-binding loop or P-loop) that includes amino acid residues 224−231 (based on the sequence of *E. coli* PriA), a DEEH motif of amino acid residues 320−323 that represents a specialized version of the Walker B motif and is thought to play a role in binding Mg^{2+}, and an element that bears resemblance to a second nucleotide-binding Walker A motif that includes amino acid residues 583−591.[22,24−26] The two Walker A motifs have been proposed to account for PriA's two nucleotide binding sites: one of which has a high affinity for nucleotides and is thought to be the primary ATP binding site and the second of which has a low affinity for binding nucleotides and is thought to be an allosteric control site.[27−29] PriA also contains a well-conserved Cys-rich element between helicase motifs IV and V that is thought to be important for zinc binding and for coupling its ATPase activity to its DNA unwinding activity.[22,30]

The types of DNA structures to which PriA can bind in vitro are highly varied. *E. coli* PriA can bind to single-stranded DNA (ssDNA), double-stranded DNA, partial duplex DNA with a 3′-ssDNA overhang, DNA fork structures with three-way branches, and D-loop structures.[31−36] While the DBD is important for binding to DNA fork structures and D-loop DNA, its affinity for DNA is lower than that of intact PriA, suggesting that binding of PriA to forked DNA structures involves contributions from both the DBD and HD.[23,37] As is true of many helicases, PriA's ATPase activity is tightly linked to its binding to a DNA lattice, and negligible levels of ATP hydrolysis are detected in the absence of DNA.[20,38] This likely reflects a tight coupling between ATP hydrolysis and translocation of the helicase along the DNA lattice, which can result in duplex DNA unwinding when a region of double-stranded DNA is encountered while the helicase translocates along the lattice.

Given the central role of PriA in bacterial DNA replication restart pathways and its importance for cell growth and viability, we sought to identify small molecule compounds that could inhibit its function. We adapted a previously described fluorescence polarization-based DNA unwinding assay for use in a high-throughput screen (HTS) to search for small molecules that could disrupt the ability of the PriA·PriB complex to catalyze unwinding of a synthetic DNA fork structure.[20] One of the hits obtained from the HTS is a triazoloquinazoline called CGS 15943. This compound had been previously identified and characterized as a potent and selective antagonist for adenosine receptors.[39,40] Here, we report that CGS 15943 functions as an inhibitor of PriA helicase activity. As the first reported small molecule inhibitor of PriA helicase, CGS 15943 could be useful for understanding mechanistic details of PriA function and for exploring the importance of PriA helicase for cell growth and survival in bacteria that rely heavily upon PriA-catalyzed DNA replication restart.

MATERIALS AND METHODS

Proteins. The *priA* and *priB* genes of *N. gonorrhoeae* strain FA1090 were cloned and the recombinant PriA and PriB proteins purified as previously described.[41] The *priA* gene of *E. coli* strain K12 was cloned and the recombinant PriA protein purified as previously described.[42] The concentrations of PriA and PriB proteins were determined by measuring their absorbance at 280 nm in 6.0 M guanidine hydrochloride using molar extinction coefficients of 78460 M^{-1} cm^{-1} for *N. gonorrhoeae* PriA, 15460 M^{-1} cm^{-1} for *N. gonorrhoeae* PriB, and 105870 M^{-1} cm^{-1} for *E. coli* PriA.[43]

Nucleic Acids. For DNA binding and unwinding assays, a fully duplex DNA fork substrate with a 3′-fluorescein-labeled nascent lagging strand arm was constructed by annealing the following partially complementary DNA oligonucleotides: template leading strand, 5′-GTC GGA TCC TCT AGA CAG CTC CAT GAT CAC TGG CAC TGG TAG AAT TCG GC; template lagging strand, 5′-ACG TAG GCC GGA AAC AAC GTC ATA GAC GAT TAC ATT GCT ACA TGG AGC TGT CTA GAG GAT CCG AC; nascent leading strand, 5′-GCC GAA TTC TAC CAG TGC CAG TGA T; nascent lagging strand with 3′-fluorescein, 5′-TAG CAA TGT AAT CGT CTA TGA CGT TGT TTC CGG CCT ACG T. The oligonucleotides were annealed in 10 mM Tris-HCl (pH 8), 50 mM NaCl, and 1 mM EDTA at a 2:1 molar ratio of nonlabeled DNA to fluorescein-labeled DNA. The DNAs were incubated at 95 °C for 5 min, slowly cooled to 70 °C, incubated at that temperature for 60 min, and slowly cooled to 25 °C. The duplex DNA was gel-purified through a 6% polyacrylamide gel using 100 mM Tris-borate (pH 8.3) and 2 mM EDTA as the electrophoresis buffer. The DNA was excised from the polyacrylamide gel, electroeluted using the same electrophoresis buffer, dialyzed against 10 mM Tris-HCl (pH 8) and 5 mM $MgCl_2$, aliquoted, and stored at −20 °C. A homopolymer dT_{36} oligonucleotide was used for steady-state enzyme kinetic experiments to measure DNA-dependent rates of PriA-catalyzed ATP hydrolysis. All oligonucleotides were purchased from Integrated DNA Technologies, Inc. (Coralville, IA).

DNA Unwinding Assay for High-Throughput Screening. The DNA unwinding assay used in high-throughput screening was performed at the University of Wisconsin Carbone Cancer Center Small Molecule Screening and Synthesis Facility using the National Institutes of Health (NIH) Clinical Collection library of 446 small molecules. The DNA fork substrate was diluted to 1 nM in 20 mM Tris-HCl

(pH 8), 50 mM NaCl, 3 mM $MgCl_2$, and 1 mM 2-mercaptoethanol and distributed into individual wells of 96-well plates. Library compounds were added at a final concentration of approximately 10 μM. Wells to which no compounds were added received an equivalent volume of dimethyl sulfoxide (DMSO) solvent. Each well received 1 mM ATP and 15 nM *N. gonorrhoeae* PriB (as monomers), and the reactions were initiated by addition of 4 nM *N. gonorrhoeae* PriA. The final volume of each reaction mixture was approximately 100 μL. The plates were incubated at 37 °C for 10 min to facilitate duplex DNA unwinding; the reactions were terminated by addition of 1% (w/v) SDS, and the fluorescence anisotropy of each well was measured at 25 °C. Fluorescence anisotropy values were compared to the fluorescence anisotropy of the DNA fork substrate incubated in buffer alone (fully intact DNA fork substrate) and the fluorescence anisotropy of the DNA fork substrate after it had been heated to 95 °C and rapidly cooled to 25 °C (fully denatured DNA substrate) to determine the fraction of DNA unwound for each experimental sample.

Determination of IC_{50}. Dose−response curves were generated by titrating CGS 15943 into mixtures of PriA and PriB proteins from either *N. gonorrhoeae* or *E. coli*. These DNA unwinding assays are similar to the one used for the HTS, except that the concentrations of PriA and PriB were varied as described in the main text to account for slight differences in enzyme activity between the two bacterial PriA homologues. In each case, the concentrations of primosome proteins were chosen to maximize the full dynamic range of the assay while avoiding saturating the assay with excess enzyme. Serial dilutions of CGS 15943 were made into DMSO from a 10 mM stock solution, and the final concentration of DMSO was fixed at 10% (v/v) for all experimental points in the CGS 15943 titrations. Fluorescence anisotropies were measured at 25 °C with a Beacon 2000 fluorescence polarization system. The concentration of CGS 15943 required for 50% inhibition (IC_{50}) was determined using a four-parameter sigmoidal model

$$y = (a - d)/[1 + (x/c)^{-b}] + d$$

where a is the minimal enzyme activity, b is the slope, c is the IC_{50}, d is the maximal enzyme activity, y is the fraction of DNA unwound, and x is the inhibitor concentration (CurveExpert version 1.3).

ATP Hydrolysis Assays. PriA·PriB complex-catalyzed ATP hydrolysis was measured using a coupled spectrophotometric assay. This assay uses an ATP regeneration system that converts ADP to ATP in a reaction that is coupled to the oxidation of NADH to NAD^+. The coupled reaction can be monitored spectrophotometrically by measuring the decrease in absorbance at 340 nm due to NADH oxidation.[44] Mixtures of 10 nM *N. gonorrhoeae* PriA and 100 nM *N. gonorrhoeae* PriB (as monomers) were incubated with indicated concentrations of dT_{36} and ATP in 20 mM Hepes (pH 8), 50 mM NaCl, 7 mM 2-mercaptoethanol, 2 mM phosphoenolpyruvate, 0.1 mM NADH, 7 units/mL pyruvate kinase, 10 units/mL lactate dehydrogenase, and 0.1 mg/mL bovine serum albumin (BSA) at 37 °C in the presence of 57 μM CGS 15943 or an equivalent volume of DMSO. Steady-state $\Delta[NADH]/\Delta t$ rates were calculated using the molar extinction coefficient of 6220 M^{-1} cm^{-1} for NADH, and these rates are equivalent to $\Delta[ATP]/\Delta t$. The kinetic parameters K_m, K_{act}, and V_{max} were determined by fitting the rates of ATP hydrolysis from individual experiments to the Michaelis−Menten equation

$$V = (V_{max}[ATP])/(K_m + [ATP])$$

for experiments in which ATP was varied or to the equation

$$V = (V_{max}[dT_{36}])/(K_{act} + [dT_{36}])$$

for experiments in which dT_{36} was varied (CurveExpert version 1.3). Values of k_{cat} were determined by dividing the apparent V_{max} by the concentration of PriA in the reaction. Reported K_m, K_{act}, and k_{cat} values are averages from at least three independent experiments, and associated uncertainty values are one standard deviation of the mean. The relationship between apparent V_{max} and K_I' was determined using the equation

$$V_{max}(app) = V_{max}/(1 + [I]/K_I')$$

The relationship among apparent K_m, K_I, and K_I' was determined using the equation

$$K_m(app) = K_m(1 + [I]/K_I)/(1 + [I]/K_I')$$

The relationship among apparent K_{act}, K_I, and K_I' was determined using the equation

$$K_{act}(app) = K_{act}(1 + [I]/K_I)/(1 + [I]/K_I')$$

Equilibrium DNA Binding Assays. CGS 15943 was titrated into a mixture of 1 nM DNA fork substrate and 10 nM *N. gonorrhoeae* PriA in a buffered solution consisting of 20 mM Tris-HCl (pH 8), 10% (v/v) glycerol, 50 mM NaCl, 1 mM 2-mercaptoethanol, and 0.1 mg/mL BSA. Serial dilutions of CGS 15943 were made into DMSO from a 10 mM stock solution, and the final concentration of DMSO was fixed at 10% (v/v) for all experimental points in the CGS 15943 titrations. The fluorescence anisotropy of the DNA fork substrate in the presence of PriA and either DMSO or a range of CGS 15943 concentrations was measured at 25 °C with a Beacon 2000 fluorescence polarization system. Following this measurement, the integrity of the DNA fork substrate was checked by adding 1% (w/v) SDS to each sample to remove bound PriA and then measuring the fluorescence anisotropy again. The unbound state of the DNA fork substrate is reported by its fluorescence anisotropy in the presence of buffer alone.

RESULTS

High-Throughput Screen for PriA·PriB Inhibitors. A fluorescence polarization-based HTS was developed to identify inhibitors of PriA·PriB complex-catalyzed duplex DNA unwinding. The HTS assay uses a fluorescently labeled DNA fork substrate that is composed of four oligonucleotides that have a combined molecular weight of 55932.5 (including the fluorescein label). The DNA strand that is covalently labeled with fluorescein at its 3′ end has a molecular weight of 12837.4 (including the fluorescein label), which is significantly smaller than the molecular weight of the intact DNA fork. Therefore, unwinding of the DNA fork substrate can be reported by a decrease in fluorescence anisotropy as the labeled DNA strand is dissociated from the remainder of the fork (Figure 1).

The HTS was performed in a 96-well plate format at the University of Wisconsin Carbone Cancer Center Small Molecule Screening and Synthesis Facility using concentrations of *N. gonorrhoeae* PriA and PriB that give approximately 60% DNA unwinding when DMSO is used as a substitute for library compounds, and the assay has a Z' factor of 0.73, indicating that the assay conditions are suitable for high-throughput screening.[45] The NIH Clinical Collection library of 446 small molecules was screened at a final concentration of approx-

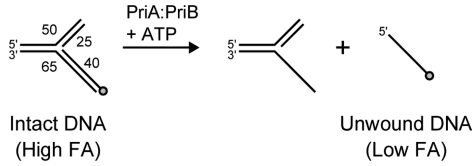

Figure 1. DNA unwinding assay for high-throughput screening. A DNA fork substrate with a 40 bp duplex 3′-fluorescein-labeled nascent lagging strand arm was incubated with PriA and PriB in the presence of ATP to facilitate DNA unwinding. Bound proteins were removed from the products using SDS, and the degree of unwinding of the 3′-fluorescein-labeled DNA strand was measured using fluorescence polarization spectroscopy. The intact DNA fork has a higher fluorescence anisotropy (FA) than the unwound products. The gray circle on the nascent lagging strand arm represents the fluorescein label, and the number adjacent to each arm of the DNA fork substrate indicates the number of base pairs in that arm of the fork.

imately 10 μM, and hits were identified as wells with a degree of duplex DNA unwinding that is at least three standard deviations below the mean level of duplex DNA unwinding for the corresponding plate's DMSO solvent control wells (of which there were eight per plate). There were five hits identified using these criteria (corresponding to approximately 1% of the library). Here, we describe the validation and characterization of one of these hits, CGS 15943.

Hit Validation and Determination of IC_{50}. From our initial HTS of the NIH Clinical Collection library, CGS 15943 produced the greatest degree of inhibition of PriA·PriB complex-catalyzed duplex DNA winding. However, given the variability that is inherent to small volume fluid transfers performed by robotic liquid handling equipment used in a HTS, we performed additional DNA unwinding assays to validate CGS 15943 as a genuine inhibitor of PriA·PriB complex-catalyzed duplex DNA unwinding. These additional assays were conducted under conditions highly similar to those used in the HTS, although a range of CGS 15943 concentrations was tested. We incubated 1 nM DNA fork substrate with 5 nM PriA and 50 nM PriB (as monomers) and either DMSO as a solvent control or CGS 15943 at concentrations ranging from 1 to 400 μM and measured the fluorescence anisotropy (Figure 2). The results of these experiments are consistent with the results of the HTS in demonstrating that CGS 15943 inhibits PriA·PriB complex-catalyzed duplex DNA unwinding. The resulting dose–response curve was modeled using a four-parameter sigmoidal model as described in Materials and Methods. The concentration of CGS 15943 that produces 50% inhibition of *N. gonorrhoeae* PriA·PriB complex-catalyzed duplex DNA unwinding (IC_{50}) under these experimental conditions is 114 ± 24 μM.

PriA Is the Target of CGS 15943-Mediated Inhibition. The DNA unwinding assay used in the HTS was designed to provide many potential points at which an inhibitor might exert its effects. An inhibitor compound could potentially disrupt DNA binding by PriA, DNA binding by PriB, PriA–PriB interactions, ATP binding or hydrolysis by PriA, or the coupling of DNA binding and ATP hydrolysis. Therefore, we sought to determine the mechanism by which CGS 15943 inhibits PriA·PriB complex-catalyzed duplex DNA unwinding. First, we investigated whether PriA, PriB, or a PriA·PriB complex is the target of inhibition. Given that PriB serves to stimulate the helicase activity of PriA, we reasoned that if CGS 15943 were to disrupt PriB function but not affect PriA, then

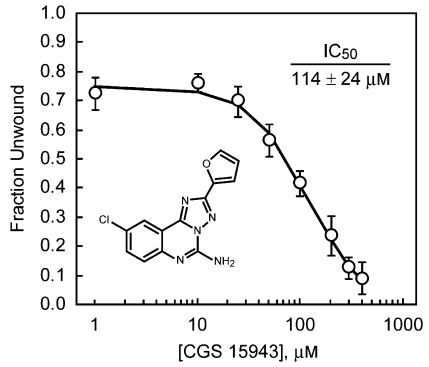

Figure 2. CGS 15943 is an inhibitor of PriA·PriB complex-catalyzed duplex DNA unwinding. Serial dilutions of CGS 15943 (structure shown in the inset) were incubated with the fluorescein-labeled DNA fork substrate in the presence of the PriA·PriB complex and ATP, and the degree of duplex DNA unwinding was measured using fluorescence polarization spectroscopy. The concentration of CGS 15943 required for 50% inhibition of duplex DNA unwinding (IC_{50}) was determined using a four-parameter sigmoidal model as described in Materials and Methods. Measurements are reported in triplicate, and error bars represent one standard deviation of the mean.

the overall levels of duplex DNA unwinding observed in the presence of inhibitor would be equivalent to the levels of duplex DNA unwinding observed for PriA alone. In the absence of both CGS 15943 and PriB, 5 nM PriA alone catalyzes the unwinding of approximately 31% of the DNA fork substrate (Figure 3). However, the titration of CGS 15943 with a mixture

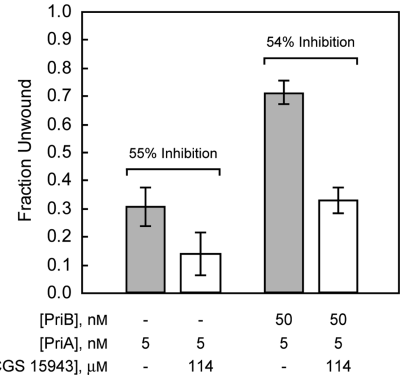

Figure 3. PriA helicase is the target of CGS 15943. The IC_{50} concentration of CGS 15943 was incubated with the fluorescein-labeled DNA fork substrate in the presence of ATP and either the PriA·PriB complex or PriA alone, and the degree of duplex DNA unwinding was measured using fluorescence polarization spectroscopy. The degree of inhibition of duplex DNA unwinding is approximately the same in the presence of PriB as it is in the absence of PriB, indicating that PriA is the target of CGS 15943-mediated inhibition. Measurements are reported in triplicate, and error bars represent one standard deviation of the mean.

of 5 nM PriA and 50 nM PriB (as monomers) demonstrates that the inhibitor is capable of reducing levels of duplex DNA unwinding to <10% at the highest concentration of CGS 15943 tested (Figure 2). The extent of maximal inhibition by CGS 15943 suggests that the inhibitor is not simply eliminating the stimulatory effects of PriB. When DNA unwinding assays are conducted using 5 nM PriA and the IC_{50} concentration of CGS 15943 in the absence of PriB, levels of duplex DNA unwinding are approximately one-half of those of the DMSO solvent

dx.doi.org/10.1021/bi301100w | *Biochemistry* 2012, 51, 10137–10146

control (Figure 3). This demonstrates that CGS 15943 is capable of exerting its inhibitory effects in the absence of PriB. Furthermore, the level of inhibition of duplex DNA unwinding exerted by CGS 15943 is approximately the same when PriB is absent (55% inhibition at 114 μM CGS 15943) as when PriB is present (54% inhibition at 114 μM CGS 15943) (Figure 3). While the relatively low level of duplex DNA unwinding that is catalyzed by PriA alone makes the inhibitory effect of CGS 15943 difficult to measure with high levels of certainty (thereby necessitating the need to include PriB in the reaction mixtures), these data suggest that PriA is the target of inhibition by CGS 15943 and that the presence of PriB is not required for CGS 15943 to function as an inhibitor.

Mechanism of CGS 15943-Mediated Inhibition. Given the structural similarity between CGS 15943 and the adenine base of ATP, we hypothesized that CGS 15943 likely functions as a competitive inhibitor of PriA by mimicking ATP and binding to the primary ATP binding site on the helicase. If this were the case, then CGS 15943 and ATP would compete with one another for binding to PriA, and any PriA helicase that has CGS 15943 bound to its primary ATP binding site would be rendered catalytically inactive and incapable of unwinding duplex DNA. To test this hypothesis, we performed steady-state enzyme kinetic experiments to measure the rate of PriA-catalyzed ATP hydrolysis in the presence and absence of CGS 15943. For competitive inhibition, we would expect to observe no change in k_{cat} and an increase in the apparent K_m in the presence of CGS 15943.

Rates of PriA-catalyzed ATP hydrolysis were measured as a function of ATP concentration and as a function of dT_{36} concentration using a spectrophotometric assay that couples ATP hydrolysis to oxidation of NADH. To measure the dependence of the rate of ATP hydrolysis on ATP concentration, we incubated 10 nM PriA and 100 nM PriB (as monomers) with 100 nM dT_{36} and various concentrations of ATP in the presence of CGS 15943 or an equivalent volume of DMSO to serve as a solvent control. In the presence of the DMSO solvent control, rates of PriA-catalyzed ATP hydrolysis show a hyperbolic dependence on the concentration of ATP, and near-maximal rates are obtained with approximately 800 μM ATP (Figure 4). These data yield a k_{cat} of 22 ± 1 s^{-1} and an apparent K_m of 79 ± 10 μM. In the presence of 57 μM CGS 15943, the k_{cat} is reduced to 14 ± 1 s^{-1} and the apparent K_m increases to 117 ± 27 μM. Thus, in the presence of CGS 15943, maximal rates of ATP hydrolysis are significantly reduced and a greater concentration of ATP is required to reach the maximal rate (Table 1). Contrary to expectations, the changes in k_{cat} and apparent K_m induced by CGS 15943 do not support a competitive mode of inhibition. Rather, the kinetic parameters suggest a mixed mode of inhibition with respect to ATP, indicating that CGS 15943 binds to PriA at a site that affects both substrate binding and catalysis but is distinct from the primary ATP binding site. The concentration of dT_{36} is saturating under these conditions; therefore, the dissociation constant, K_I, should reflect binding of the inhibitor to the PriA·PriB·dT_{36} complex, and the dissociation constant, K_I', should reflect binding of the inhibitor to the PriA·PriB·dT_{36}·ATP complex. Under these conditions, K_I is 52 ± 24 μM and K_I' is 103 ± 6 μM.

To measure the dependence of the rate of ATP hydrolysis on DNA concentration, we incubated 10 nM PriA and 100 nM PriB (as monomers) with 1 mM ATP and various concentrations of dT_{36} in the presence of CGS 15943 or an equivalent volume of DMSO to serve as a solvent control. In the presence of the DMSO solvent control, rates of PriA-catalyzed ATP hydrolysis show a hyperbolic dependence on the concentration of dT_{36}, and near-maximal rates are obtained with approximately 100 nM dT_{36} (Figure 5). These data yield a k_{cat} of 22 ± 1 s^{-1} and an apparent K_{act} of 7 ± 1 nM. In the presence of 57 μM CGS 15943, the k_{cat} is reduced to 14 ± 4 s^{-1} and the apparent K_{act} increases to 42 ± 26 nM. Thus, maximal rates of ATP hydrolysis are significantly reduced, and a greater concentration of dT_{36} is required to reach the maximal rate in the presence of CGS 15943 (Table 1). These kinetic parameters suggest a mixed mode of inhibition with respect to DNA. The concentration of ATP is saturating under these conditions; therefore, the dissociation constant, K_I, should reflect binding of the inhibitor to the PriA·PriB·ATP complex, and the dissociation constant, K_I', should reflect binding of the inhibitor to the PriA·PriB·dT_{36}·ATP complex. Under these conditions, K_I is 9 ± 4 μM and K_I' is 125 ± 87 μM.

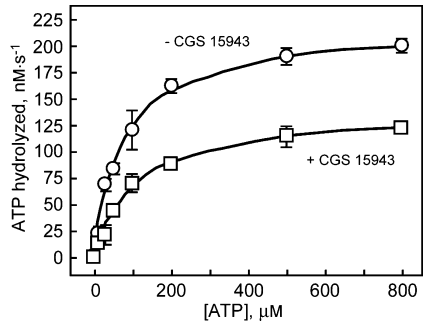

Figure 4. CGS 15943 exerts a mixed mode of inhibition with respect to ATP. Steady-state rates of PriA·PriB complex-catalyzed ATP hydrolysis were measured using 100 nM dT_{36} and various concentrations of ATP in the presence and absence of 57 μM CGS 15943 as described in Materials and Methods. Measurements are reported in triplicate, and error bars represent one standard deviation of the mean. The best-fit curves were generated by fitting the averaged data from triplicate experiments to the Michaelis–Menten equation [$V = (V_{max}[ATP])/(K_m + [ATP])$] and are shown here for illustrative purposes only.

Table 1. Kinetic Parameters for PriA·PriB Complex-Catalyzed ATP Hydrolysis in the Presence and Absence of CGS 15943[a]

	ATP titration		dT_{36} titration	
	DMSO control	CGS 15943	DMSO control	CGS 15943
K_m(app) (μM)	79 ± 10	117 ± 27	N/A[b]	N/A[b]
K_{act}(app) (nM)	N/A[b]	N/A[b]	7 ± 1	42 ± 26
k_{cat} (s^{-1})	22 ± 1	14 ± 1	22 ± 1	14 ± 4
K_I (μM)		52 ± 24		9 ± 4
K_I' (μM)		103 ± 6		125 ± 87

[a]Kinetic parameters are mean values derived from at least three independent experiments, and associated uncertainty values are one standard deviation of the mean. For the ATP titrations, K_I is the inhibitor dissociation constant that describes binding of CGS 15943 to the PriA·PriB·dT_{36} complex and K_I' is the inhibitor dissociation constant that describes binding of CGS 15943 to the PriA·PriB·dT_{36}·ATP complex. For the dT_{36} titrations, K_I is the inhibitor dissociation constant that describes binding of CGS 15943 to the PriA·PriB·ATP complex and K_I' is the inhibitor dissociation constant that describes binding of CGS 15943 to the PriA·PriB·dT_{36}·ATP complex. [b]Not applicable.

dx.doi.org/10.1021/bi301100w | Biochemistry 2012, 51, 10137–10146

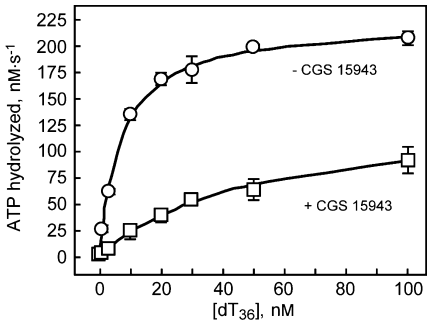

Figure 5. CGS 15943 exerts a mixed mode of inhibition with respect to DNA. Steady-state rates of PriA·PriB complex-catalyzed ATP hydrolysis were measured using 1 mM ATP and various concentrations of dT_{36} in the presence and absence of 57 μM CGS 15943 as described in Materials and Methods. Measurements are reported in triplicate, and error bars represent one standard deviation of the mean. The best-fit curves were generated by fitting the averaged data from triplicate experiments to the Michaelis–Menten equation [$V = (V_{max}[dT_{36}])/(K_{act} + [dT_{36}])$] and are shown here for illustrative purposes only.

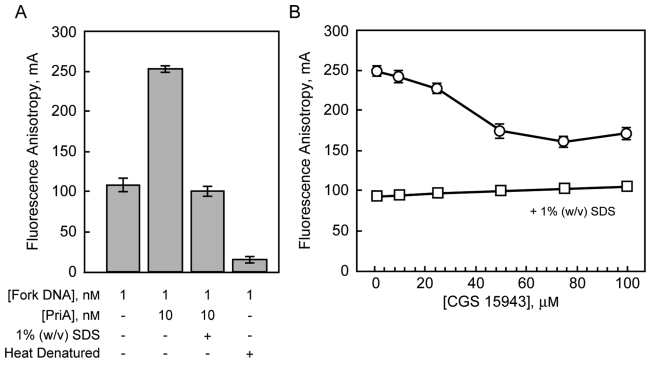

Figure 6. CGS 15943 affects stable DNA binding by PriA. (A) The fluorescein-labeled DNA fork substrate was incubated with PriA in the absence of ATP to form a PriA·DNA complex. Complex formation was monitored by measuring the fluorescence anisotropy of the labeled DNA in the presence and absence of PriA. Addition of 1% (w/v) SDS facilitates dissociation of the PriA·DNA complex, and the measured fluorescence anisotropy reveals that the DNA fork is not unwound by PriA in the absence of ATP. Measurements are reported in triplicate, and error bars represent one standard deviation of the mean. (B) Serial dilutions of CGS 15943 were incubated with the fluorescein-labeled DNA fork substrate in the presence of PriA, and the degree of PriA·DNA complex formation was measured using fluorescence polarization spectroscopy. Subsequent addition of 1% (w/v) SDS to the samples results in dissociation of the PriA·DNA complex, and the measured fluorescence anisotropy reveals that neither PriA nor CGS 15943 results in duplex DNA unwinding under these experimental conditions. Thus, the CGS 15943-mediated decrease in the fluorescence anisotropy of the PriA·DNA complex is likely caused by a decrease in the level of stable DNA binding by PriA. Measurements are reported in triplicate, and error bars represent one standard deviation of the mean.

In the ATP hydrolysis assays described above, the concentration of CGS 15943 is one-half of the IC_{50} that was defined on the basis of duplex DNA unwinding. When the IC_{50} concentration of CGS 15943 is used in the ATP hydrolysis experiments, levels of ATP hydrolysis are very low (significantly less than one-half of DMSO solvent control levels) and difficult to measure with certainty. The discrepancy between observed levels of inhibition of duplex DNA unwinding and observed levels of inhibition of ATP hydrolysis at the IC_{50} concentration of CGS 15943 could be due to the different DNA substrates used to measure these activities: the duplex DNA unwinding assays use a DNA fork substrate, while the ATP hydrolysis assays use a dT homopolymer as a substrate. The observed differences could indicate that different conformations of PriA exist when the helicase engages a DNA fork substrate than when it binds a region of ssDNA. The dT homopolymer was used as a substrate in the ATP hydrolysis assays, as opposed to a duplex DNA substrate, to avoid the potential issue of having mixtures of duplex DNA and unwound single-stranded DNA form throughout the course of the experiment. The use of a dT homopolymer ensures a homogeneous template for stimulating PriA-catalyzed ATP hydrolysis.

Given that CGS 15943 causes an increase in PriA's apparent K_{act}, we examined the effect of CGS 15943 on stable DNA binding by PriA using an equilibrium DNA binding assay. For these experiments, we formed a PriA·DNA complex by incubating 1 nM DNA fork substrate with 10 nM PriA. As expected, the PriA·DNA complex has a higher fluorescence anisotropy (approximately 250 mA) than does the free DNA fork substrate (approximately 100 mA) (Figure 6A). Removal of bound PriA by addition of 1% (w/v) SDS reduces the fluorescence anisotropy back to levels observed for the free DNA fork substrate, indicating that PriA does not permanently modify the DNA fork substrate under these experimental conditions. To determine if CGS 15943 affects stable DNA binding by PriA, we titrated CGS 15943 into solutions containing the PriA·DNA complex and measured the resulting fluorescence anisotropy. We observed a CGS 15943-dependent decrease in fluorescence anisotropy from approximately 250 mA in the absence of CGS 15943 to approximately 160 mA in the presence of 75 μM CGS 15943 (Figure 6B). The fluorescence anisotropy does not change significantly with an increase in the concentration of CGS 15943 to 100 μM. Even though CGS 15943 does not reduce the fluorescence anisotropy to levels observed for the completely unbound DNA fork, these data suggest that binding of CGS 15943 to PriA disrupts PriA's ability to bind DNA.

To ensure that the CGS 15943-dependent decrease in fluorescence anisotropy is not due to unwinding of the DNA fork substrate, the samples were incubated with 1% (w/v) SDS after the initial fluorescence anisotropy reading to remove bound PriA, and the fluorescence anisotropy was measured again. The SDS treatment reduces the fluorescence anisotropy of the CGS 15943 titration samples to the level observed for the DNA fork substrate in buffer alone (Figure 6). This indicates that the DNA fork substrate is not being unwound under these experimental conditions. Thus, the CGS 15943-dependent decrease in fluorescence anisotropy is likely due to dissociation of the PriA·DNA complex.

Species Specificity of CGS 15943-Mediated PriA Inhibition. While our HTS for inhibitors of PriA·PriB complex-catalyzed duplex DNA unwinding made use of *N. gonorrhoeae* DNA replication restart primosome proteins, we wanted to determine if CGS 15943 would disrupt the function of PriA from other bacterial species. Therefore, we tested the ability of CGS 15943 to inhibit duplex DNA unwinding catalyzed by *E. coli* PriA using an experimental setup that is similar to the one used to study *N. gonorrhoeae* PriA and PriB. Because our work with the *N. gonorrhoeae* DNA replication restart primosome proteins reveals that CGS 15943 targets PriA, for these experiments we chose to examine the DNA

unwinding activity of *E. coli* PriA without its cognate PriB protein. We performed DNA unwinding assays using 1 nM DNA fork substrate and 5 nM *E. coli* PriA in the presence of either DMSO as a solvent control or CGS 15943 at concentrations ranging from 1 to 400 μM. We observed a CGS 15943-dependent decrease in the level of *E. coli* PriA-catalyzed duplex DNA unwinding (Figure 7). The resulting

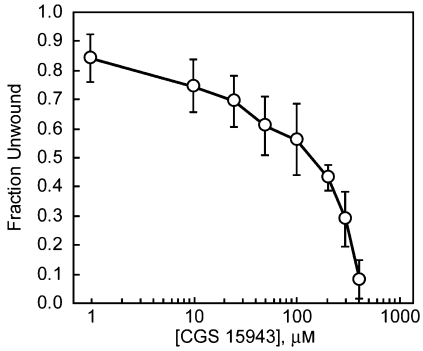

Figure 7. *E. coli* PriA helicase is inhibited by CGS 15943. Serial dilutions of CGS 15943 were incubated with the fluorescein-labeled DNA fork substrate in the presence of PriA and ATP, and the degree of duplex DNA unwinding was measured using fluorescence polarization spectroscopy. Measurements are reported in triplicate, and error bars represent one standard deviation of the mean.

dose−response curve lacks a lower baseline and cannot be modeled using the four-parameter sigmoidal model that was used to determine the IC_{50} for CGS 15943-mediated inhibition of the *N. gonorrhoeae* PriA and PriB proteins. Thus, we are unable to determine the IC_{50} value for CGS 15943-mediated inhibition of *E. coli* PriA. It is clear, however, that CGS 15943 has an inhibitory effect on *E. coli* PriA, albeit an effect weaker than that observed for *N. gonorrhoeae* PriA.

DISCUSSION

In this study, we have adapted a fluorescence polarization-based DNA unwinding assay for use in HTS to identify small molecule inhibitors of PriA helicase activity. Our initial HTS of the 446-compound NIH Clinical Collection library yielded a hit, CGS 15943, that we have verified to be an inhibitor of PriA-catalyzed duplex DNA unwinding. While our HTS assay includes both PriA and PriB, we have determined that CGS 15943 targets PriA and does so in a manner that does not require the presence of PriB. Furthermore, the inhibitory effects of CGS 15943 are not restricted to primosome proteins from the bacterial species whose PriA and PriB proteins were used in HTS. While the HTS made use of *N. gonorrhoeae* PriA and PriB proteins, we have found that *E. coli* PriA is also inhibited by CGS 15943. Thus, the binding site on PriA that is targeted by CGS 15943 is likely a fairly well-conserved structural feature of the enzyme.

Given the high degree of structural similarity between CGS 15943 and the adenine base of ATP, we hypothesized that CGS 15943 exerts its inhibition of PriA-catalyzed duplex DNA unwinding by mimicking ATP and binding to the primary ATP binding site on the helicase, thereby restricting PriA's access to ATP. Because ATP binding and hydrolysis are necessary to promote PriA-catalyzed duplex DNA unwinding, any direct competition between ATP and another small molecule would lead to diminished levels of DNA unwinding.[15,16] From our investigation into the mechanism of CGS 15943-mediated inhibition of PriA, we have demonstrated that CGS 15943 decreases the steady-state maximal velocity of PriA-catalyzed ATP hydrolysis and increases K_m and K_{act}. The steady-state kinetic analysis indicates that CGS 15943 exhibits a mixed mode of inhibition with respect to ATP and with respect to DNA. This implies that CGS 15943 binds to PriA at a site that is distinct from the primary ATP and DNA binding sites and presumably blocks necessary conformational changes in the helicase or distorts the conformation of the helicase in a manner that makes it less conducive to binding DNA and ATP and coupling ATP hydrolysis to duplex DNA unwinding. Helicases in general are thought to undergo conformational changes as they hydrolyze ATP and unwind duplex nucleic acids, and the differences in the measured equilibrium constants for binding of CGS 15943 to the PriA·PriB·dT_{36} complex, the PriA·PriB·ATP complex, and the PriA·PriB·dT_{36}·ATP complex provide indirect evidence that conformational changes do indeed accompany binding of DNA and ATP to PriA.

While the exact location where CGS 15943 binds to PriA has not yet been established, the features of the PriA−CGS 15943 interaction that we report in this study appear to be consistent with a model in which CGS 15943 binds to the weak nucleotide binding site on PriA that has previously been biochemically defined and characterized.[27−29] The weak nucleotide binding site has been shown to have modest base specificity compared to that of the strong nucleotide binding site, which shows a preference for adenosine coenzymes.[27] It is possible that this modest base specificity translates into a sufficient degree of structural and chemical complementarity to accommodate CGS 15943, particularly given the structural similarity between CGS 15943 and the adenine base of ATP. Furthermore, the weak nucleotide binding site has been shown to be an allosteric control site on PriA that influences PriA's interactions with DNA.[28,29] For example, when the weak nucleotide binding site is bound by the nonhydrolyzable ATP analogue, ATPγS, and the strong nucleotide binding site is bound by ATPγS or ADP, the affinity of PriA for ssDNA is diminished.[29] This indicates direct communication between the weak nucleotide binding site and the primary DNA binding site on PriA. Were CGS 15943 to bind to such an allosteric control site, it would be reasonable to expect perturbations to PriA's DNA binding activity such as those observed for ATPγS. The observation that CGS 15943 disrupts stable DNA fork binding by PriA would therefore support the hypothesis that CGS 15943 binds to the weak nucleotide binding site on PriA. However, locating the exact CGS 15943 binding site on PriA, as well as mapping the physical location of PriA's weak nucleotide binding site, will likely require a high-resolution model of PriA helicase, which, at present, is a goal that has not yet been realized.

PriA is not the first helicase to be targeted for inhibition by screening libraries of small molecule compounds. Indeed, a variety of cellular and viral helicases have been the subject of small molecule inhibitor screening studies, many of which have been performed to identify compounds that are promising drug candidates as well as to provide insight into the mechanistic function of the helicases being targeted.[46] For example, a small molecule compound from the National Cancer Institute Diversity Set (NSC 19630) has been identified as an inhibitor of WRN helicase, a human homologue of the bacterial RecQ helicase.[47] This compound is specific for inhibiting WRN helicase compared to other human and bacterial helicases and reduces overall levels of DNA unwinding by a significant degree (75% inhibition of DNA unwinding at 50 μM) while having an

only modest effect on rates of ATP hydrolysis (19% reduction in k_{cat} for ATP hydrolysis at 50 μM).[47] These observations could indicate that NSC 19630 affects the coupling of ATP hydrolysis to duplex DNA unwinding for WRN helicase.

The helicase component (UL5) of the herpes simplex virus (HSV) helicase−primase complex (UL5−UL8−UL52) has also been the target of small molecule inhibitor screens, because of the importance of this complex for viral replication. In this case, numerous small molecule inhibitors have been identified, including several amino-thiazolylphenyl compounds, thiazole urea compounds, and thiazole amide compounds, that all appear to enhance binding of the UL5 and UL52 subunits of the helicase−primase complex to the DNA, resulting in inhibition of both helicase and primase activity by blocking progression through the helicase and primase catalytic cycles.[48−51] In addition, (dichloroanilino)purines and -pyrimidines have been shown to inhibit NTP hydrolysis and duplex DNA unwinding by the HSV helicase−primase complex, likely by binding to the NTP binding site on the surface of the helicase.[52]

Small molecule inhibitors that target the NS3 helicase of hepatitis C virus have also been identified. Mechanisms of action for these helicase inhibitors include competitive inhibition with respect to NTP binding, noncompetitive inhibition that suggests allosteric effects of the inhibitor on the helicase, disruption of duplex nucleic acid unwinding without affecting rates of NTP hydrolysis (suggesting that the inhibitors affect the coupling of NTP hydrolysis to duplex nucleic acid unwinding), and competitive inhibition with respect to nucleic acid binding.[53] The IC_{50} values for these structurally diverse helicase inhibitors range from the low micromolar to millimolar range, likely reflecting a wide range of binding affinities between the helicase and inhibitor, and a wide range of mechanisms by which they inhibit.[53]

What these helicase inhibitor studies generally reveal is that helicases offer multiple potential mechanisms of action by which a small molecule inhibitor can exert its effects, reflecting the multiple enzymatic activities that are involved in binding nucleoside triphosphates and nucleic acids, and coupling the hydrolysis of an NTP to the unwinding of a duplex DNA or RNA. In our study, we have investigated the inhibitory effects of CGS 15943 on the helicase activity of PriA and concluded that the most likely mechanism by which the inhibitor acts is by binding to PriA at an allosteric control site in a way that renders PriA less capable of binding DNA and ATP and coupling ATP hydrolysis to duplex DNA unwinding. Because CGS 15943 is but the first small molecule PriA inhibitor to be identified by our HTS and verified, it is likely that further screening will reveal additional compounds that inhibit PriA, and perhaps compounds that act with greater potency or inhibit PriA by alternate mechanisms await discovery.

AUTHOR INFORMATION

Corresponding Author

*Telephone: (937) 229-2674. Fax: (937) 229-2635. E-mail: mlopper1@udayton.edu.

Author Contributions

The manuscript was written through contributions of all authors. All authors have given approval to the final version of the manuscript.

Funding

This work was supported by a grant from Research Corporation for Science Advancement to M.E.L. and by grants from the University of Dayton Graduate School to B.S. and L.B.

Notes

The authors declare no competing financial interest.

ACKNOWLEDGMENTS

We thank Madeleine A. P. DeBeer for critical review of the manuscript.

ABBREVIATIONS

ssDNA, single-stranded DNA; HTS, high-throughput screening; K_m, ATP concentration at $^1/_2V_{max}$; K_{act}, dT concentration at $^1/_2V_{max}$; DMSO, dimethyl sulfoxide; NTP, nucleoside 5′-triphosphate; dT, deoxythymidylate; FA, fluorescence anisotropy; SDS, sodium dodecyl sulfate; HSV, herpes simplex virus; Tris, tris(hydroxymethyl)aminomethane; EDTA, ethylenediaminetetraacetic acid; BSA, bovine serum albumin; Hepes, 4-(2-hydroxyethyl)piperazine-1-ethanesulfonic acid.

REFERENCES

(1) Cox, M. M., Goodman, M. F., Kreuzer, K. N., Sherratt, D. J., Sandler, S. J., and Marians, K. J. (2000) The importance of repairing stalled replication forks. *Nature 404* (6773), 37−41.

(2) Heller, R. C., and Marians, K. J. (2006) Replisome assembly and the direct restart of stalled replication forks. *Nat. Rev. Mol. Cell Biol. 7* (12), 932−943.

(3) Sandler, S. J. (2000) Multiple genetic pathways for restarting DNA replication forks in *Escherichia coli* K-12. *Genetics 155* (2), 487−497.

(4) McCool, J. D., Ford, C. C., and Sandler, S. J. (2004) A dnaT mutant with phenotypes similar to those of a priA2::kan mutant in *Escherichia coli* K-12. *Genetics 167* (2), 569−578.

(5) Sandler, S. J., Marians, K. J., Zavitz, K. H., Coutu, J., Parent, M. A., and Clark, A. J. (1999) dnaC mutations suppress defects in DNA replication- and recombination-associated functions in priB and priC double mutants in *Escherichia coli* K-12. *Mol. Microbiol. 34* (1), 91−101.

(6) Heller, R. C., and Marians, K. J. (2005) The Disposition of Nascent Strands at Stalled Replication Forks Dictates the Pathway of Replisome Loading during Restart. *Mol. Cell 17* (5), 733−743.

(7) Sandler, S. J., McCool, J. D., Do, T. T., and Johansen, R. U. (2001) PriA mutations that affect PriA-PriC function during replication restart. *Mol. Microbiol. 41* (3), 697−704.

(8) Nurse, P., Zavitz, K. H., and Marians, K. J. (1991) Inactivation of the *Escherichia coli* priA DNA replication protein induces the SOS response. *J. Bacteriol. 173* (21), 6686−6693.

(9) Grompone, G., Ehrlich, S. D., and Michel, B. (2003) Replication restart in gyrB *Escherichia coli* mutants. *Mol. Microbiol. 48* (3), 845−854.

(10) Flores, M. J., Ehrlich, S. D., and Michel, B. (2002) Primosome assembly requirement for replication restart in the *Escherichia coli* holDG10 replication mutant. *Mol. Microbiol. 44* (3), 783−792.

(11) Kline, K. A., and Seifert, H. S. (2005) Mutation of the priA Gene of *Neisseria gonorrhoeae* Affects DNA Transformation and DNA Repair. *J. Bacteriol. 187* (15), 5347−5355.

(12) Tala, A., De Stefano, M., Bucci, C., and Alifano, P. (2008) Reverse transcriptase-PCR differential display analysis of meningococcal transcripts during infection of human cells: Up-regulation of priA and its role in intracellular replication. *BMC Microbiol. 8* (1), 131.

(13) McGlynn, P., Al-Deib, A. A., Liu, J., Marians, K. J., and Lloyd, R. G. (1997) The DNA replication protein PriA and the recombination protein RecG bind D-loops. *J. Mol. Biol. 270* (2), 212−221.

(14) Ng, J. Y., and Marians, K. J. (1996) The ordered assembly of the ϕX174-type primosome. I. Isolation and identification of intermediate protein-DNA complexes. *J. Biol. Chem. 271* (26), 15642−15648.
(15) Lee, M. S., and Marians, K. J. (1987) *Escherichia coli* replication factor Y, a component of the primosome, can act as a DNA helicase. *Proc. Natl. Acad. Sci. U.S.A. 84* (23), 8345−8349.
(16) Lasken, R. S., and Kornberg, A. (1988) The primosomal protein n′ of *Escherichia coli* is a DNA helicase. *J. Biol. Chem. 263* (12), 5512−5518.
(17) Allen, G. C., Jr., and Kornberg, A. (1993) Assembly of the primosome of DNA replication in *Escherichia coli*. *J. Biol. Chem. 268* (26), 19204−19209.
(18) Cadman, C. J., Lopper, M., Moon, P. B., Keck, J. L., and McGlynn, P. (2005) PriB stimulates PriA helicase via an interaction with single-stranded DNA. *J. Biol. Chem. 280* (48), 39693−39700.
(19) Liu, J., Nurse, P., and Marians, K. J. (1996) The ordered assembly of the ϕX174-type primosome. III. PriB facilitates complex formation between PriA and DnaT. *J. Biol. Chem. 271* (26), 15656−15661.
(20) Feng, C., Sunchu, B., Greenwood, M. E., and Lopper, M. E. (2011) A bacterial PriB with weak single-stranded DNA binding activity can stimulate the DNA unwinding activity of its cognate PriA helicase. *BMC Microbiol. 11*, 189.
(21) Gorbalenya, A. E., and Koonin, E. V. (1993) Helicases: Amino acid sequence comparisons and structure-function relationships. *Curr. Opin. Struct. Biol. 3* (3), 419−429.
(22) Nurse, P., DiGate, R. J., Zavitz, K. H., and Marians, K. J. (1990) Molecular cloning and DNA sequence analysis of *Escherichia coli* priA, the gene encoding the primosomal protein replication factor Y. *Proc. Natl. Acad. Sci. U.S.A. 87* (12), 4615−4619.
(23) Tanaka, T., Mizukoshi, T., Taniyama, C., Kohda, D., Arai, K., and Masai, H. (2002) DNA Binding of PriA Protein Requires Cooperation of the N-terminal D-loop/Arrested-fork Binding and C-terminal Helicase Domains. *J. Biol. Chem. 277* (41), 38062−38071.
(24) Linder, P., Lasko, P. F., Ashburner, M., Leroy, P., Nielsen, P. J., Nishi, K., Schnier, J., and Slonimski, P. P. (1989) Birth of the D-E-A-D box. *Nature 337* (6203), 121−122.
(25) Walker, J. E., Saraste, M., Runswick, M. J., and Gay, N. J. (1982) Distantly related sequences in the α- and β-subunits of ATP synthase, myosin, kinases and other ATP-requiring enzymes and a common nucleotide binding fold. *EMBO J. 1* (8), 945−951.
(26) Brosh, R. M., Jr., and Matson, S. W. (1995) Mutations in motif II of *Escherichia coli* DNA helicase II render the enzyme nonfunctional in both mismatch repair and excision repair with differential effects on the unwinding reaction. *J. Bacteriol. 177* (19), 5612−5621.
(27) Lucius, A. L., Jezewska, M. J., and Bujalowski, W. (2006) The *Escherichia coli* PriA helicase has two nucleotide-binding sites differing dramatically in their affinities for nucleotide cofactors. 1. Intrinsic affinities, cooperativities, and base specificity of nucleotide cofactor binding. *Biochemistry 45* (23), 7202−7216.
(28) Lucius, A. L., Jezewska, M. J., Roychowdhury, A., and Bujalowski, W. (2006) Kinetic mechanisms of the nucleotide cofactor binding to the strong and weak nucleotide-binding site of the *Escherichia coli* PriA helicase. 2. *Biochemistry 45* (23), 7217−7236.
(29) Lucius, A. L., Jezewska, M. J., and Bujalowski, W. (2006) Allosteric interactions between the nucleotide-binding sites and the ssDNA-binding site in the PriA helicase-ssDNA complex. 3. *Biochemistry 45* (23), 7237−7255.
(30) Zavitz, K. H., and Marians, K. J. (1993) Helicase-deficient cysteine to glycine substitution mutants of *Escherichia coli* replication protein PriA retain single-stranded DNA-dependent ATPase activity. Zn^{2+} stimulation of mutant PriA helicase and primosome assembly activities. *J. Biol. Chem. 268* (6), 4337−4346.
(31) Liu, J., and Marians, K. J. (1999) PriA-directed assembly of a primosome on D loop DNA. *J. Biol. Chem. 274* (35), 25033−25041.
(32) Jones, J. M., and Nakai, H. (1999) Duplex opening by primosome protein PriA for replisome assembly on a recombination intermediate. *J. Mol. Biol. 289* (3), 503−516.
(33) Nurse, P., Liu, J., and Marians, K. J. (1999) Two modes of PriA binding to DNA. *J. Biol. Chem. 274* (35), 25026−25032.
(34) Jezewska, M. J., and Bujalowski, W. (2000) Interactions of *Escherichia coli* replicative helicase PriA protein with single-stranded DNA. *Biochemistry 39* (34), 10454−10467.
(35) Jezewska, M. J., Rajendran, S., and Bujalowski, W. (2000) *Escherichia coli* replicative helicase PriA protein-single-stranded DNA complex. Stoichiometries, free energy of binding, and cooperativities. *J. Biol. Chem. 275* (36), 27865−27873.
(36) Mizukoshi, T., Tanaka, T., Arai, K., Kohda, D., and Masai, H. (2003) A critical role of the 3′ terminus of nascent DNA chains in recognition of stalled replication forks. *J. Biol. Chem. 278* (43), 42234−42239.
(37) Chen, H. W., North, S. H., and Nakai, H. (2004) Properties of the PriA helicase domain and its role in binding PriA to specific DNA structures. *J. Biol. Chem. 279* (37), 38503−38512.
(38) Wickner, S., and Hurwitz, J. (1975) Association of ϕX174 DNA-dependent ATPase activity with an *Escherichia coli* protein, replication factor Y, required for in vitro synthesis of ϕX174 DNA. *Proc. Natl. Acad. Sci. U.S.A. 72* (9), 3342−3346.
(39) Ghai, G., Francis, J. E., Williams, M., Dotson, R. A., Hopkins, M. F., Cote, D. T., Goodman, F. R., and Zimmerman, M. B. (1987) Pharmacological characterization of CGS 15943A: A novel non-xanthine adenosine antagonist. *J. Pharmacol. Exp. Ther. 242* (3), 784−790.
(40) Williams, M., Francis, J., Ghai, G., Braunwalder, A., Psychoyos, S., Stone, G. A., and Cash, W. D. (1987) Biochemical characterization of the triazoloquinazoline, CGS 15943, a novel, non-xanthine adenosine antagonist. *J. Pharmacol. Exp. Ther. 241* (2), 415−420.
(41) Dong, J., George, N. P., Duckett, K. L., DeBeer, M. A., and Lopper, M. E. (2009) The crystal structure of *Neisseria gonorrhoeae* PriB reveals mechanistic differences among bacterial DNA replication restart pathways. *Nucleic Acids Res. 38* (2), 499−509.
(42) Lopper, M., Boonsombat, R., Sandler, S. J., and Keck, J. L. (2007) A hand-off mechanism for primosome assembly in replication restart. *Mol. Cell 26* (6), 781−793.
(43) Edelhoch, H. (1967) Spectroscopic determination of tryptophan and tyrosine in proteins. *Biochemistry 6* (7), 1948−1954.
(44) Morrical, S. W., Lee, J., and Cox, M. M. (1986) Continuous association of *Escherichia coli* single-stranded DNA binding protein with stable complexes of recA protein and single-stranded DNA. *Biochemistry 25* (7), 1482−1494.
(45) Zhang, J. H., Chung, T. D., and Oldenburg, K. R. (1999) A Simple Statistical Parameter for Use in Evaluation and Validation of High Throughput Screening Assays. *J. Biomol. Screening 4* (2), 67−73.
(46) Kwong, A. D., Rao, B. G., and Jeang, K. T. (2005) Viral and cellular RNA helicases as antiviral targets. *Nat. Rev. Drug Discovery 4* (10), 845−853.
(47) Aggarwal, M., Sommers, J. A., Shoemaker, R. H., and Brosh, R. M., Jr. (2011) Inhibition of helicase activity by a small molecule impairs Werner syndrome helicase (WRN) function in the cellular response to DNA damage or replication stress. *Proc. Natl. Acad. Sci. U.S.A. 108* (4), 1525−1530.
(48) Crute, J. J., Grygon, C. A., Hargrave, K. D., Simoneau, B., Faucher, A.-M., Bolger, G., Kibler, P., Liuzzi, M., and Cordingley, M. G. (2002) Herpes simplex virus helicase-primase inhibitors are active in animal models of human disease. *Nat. Med. 8* (4), 386−391.
(49) Kleymann, G., Fischer, R., Betz, U. A., Hendrix, M., Bender, W., Schneider, U., Handke, G., Eckenberg, P., Hewlett, G., Pevzner, V., Baumeister, J., Weber, O., Henninger, K., Keldenich, J., Jensen, A., Kolb, J., Bach, U., Popp, A., Maben, J., Frappa, I., Haebich, D., Lockhoff, O., and Rubsamen-Waigmann, H. (2002) New helicase-primase inhibitors as drug candidates for the treatment of herpes simplex disease. *Nat. Med. 8* (4), 392−398.
(50) Spector, F. C., Liang, L., Giordano, H., Sivaraja, M., and Peterson, M. G. (1998) Inhibition of herpes simplex virus replication by a 2-amino thiazole via interactions with the helicase component of the UL5-UL8-UL52 complex. *J. Virol. 72* (9), 6979−6987.

(51) Kleymann, G. (2004) Helicase primase: Targeting the Achilles heel of herpes simplex viruses. *Antiviral Chem. Chemother. 15* (3), 135−140.
(52) Crute, J. J., Lehman, I. R., Gambino, J., Yang, T. F., Medveczky, P., Medveczky, M., Khan, N. N., Mulder, C., Monroe, J., and Wright, G. E. (1995) Inhibition of herpes simplex virus type 1 helicase-primase by (dichloroanilino)purines and -pyrimidines. *J. Med. Chem. 38* (10), 1820−1825.
(53) Borowski, P., Schalinski, S., and Schmitz, H. (2002) Nucleotide triphosphatase/helicase of hepatitis C virus as a target for antiviral therapy. *Antiviral Res. 55* (3), 397−412.